A Numerical Procedure for Defogging Process Simulation in Automotive Industry

G. CROCE[1], P. D'AGARO[1], F. MATTIELLO[2], A. DE ANGELIS[1],
[1]DiEM, Dipartimento di Energetica e Macchine
Università di Udine,
Via delle Scienze 208, 33100
ITALY

[2] Centro Ricerche Fiat
Orbassano (TO)
ITALY

Abstract: - A suite of routines for the prediction of environment moist condensation and evaporation on solid surfaces is presented. The physical problems requires the solution of the air flow field along a (cold) solid surface, the evaluation of the unsteady conduction through the solid itself, and the development of a suitable model for the heat and mass transfer through the thin water layer on the fogged surface. The routines for the unsteady simulation of the water layer evolution are designed as a purely interfacial procedure, minimising the exchange of information with both the flow and the conductive solver. This allows the coupling with different solvers. Here, the model is used in connection with a commercial CFD solver, in order to predict the defogging process of a car windshield. The water layer is modelled as a collection of closely packed tiny droplets, leaving a portion of dry area among them. The effect of the contact angle is taken into account, and physical assumptions allow to define the local ratio between wet and dry surface for both the fogging and defogging process..

Key-Words: - Fogging, defogging, windshield, conjugate heat transfer, droplet, evaporation, condensation

1 Introduction

Cold glass fogging and the related reduction of visibility is a major concern for several industrial applications. For instance, the certification processes in automotive or aeronautic industry require quick windshield defogging, ensuring adequate visibility and preserving passenger safety.

A typical problem for the commercial refrigeration industry is the optimization of glass door demisting in closed display cabinets: when the door is open, in fact, condensation of the atmospheric humidity takes place on its cold glass surface, and quick defogging must be achieved to ensure proper visibility through the glass. Electric heaters embedded in the glass are commonly used in such situations. Unfortunately, they yield undesired energy consumption, due both to their heat release and to the refrigeration system power required to remove such heat. Thus, these systems need careful designed and the understanding and prediction of condensation-evaporation is an essential step of such a design process. Similar problem occurs when spectacle glasses get fogged as soon as a person quickly moves from a cold to a warm environment. Low thermal capacity glasses or proper coatings may reduce the inconvenience, and we should understand the effect of surface wettability in order to evaluate the coating performances.

Physically, dew or glass fogging occurs when condensation of environment air humidity takes place on a cold surface. This creates a complex tiny droplet pattern on the glass surface, leaving small portions of dry surface; light scattering due to these droplets reduces visibility through the glass. During the defogging process these droplets will evaporate. Thus, all of the above mentioned phenomena are essentially conjugate fluid-solid heat transfer problems in presence of a phase changing fluid layer on the interface. In such conditions, and the evaporation latent heat plays a significant role.

Since the region where phase change takes place is limited to a thin layer on the solid surface, we use standard single phase flow solvers for the main flow analysis. The coupling between water layer evolution and flow field depends upon the heat transfer mechanism. For thermally driven flows, as

in the case of spectacle lenses, the phase change evolution is fully coupled with both the solid conduction and the fluid dynamic simulation, due to latent heat release. On the other hand, in forced convection devices we could have a complete decoupling. The actual droplet size and wet-dry area ratio may affect both the active surface for heat and mass transfer and define the actual light scattering.

A huge amount theoretical and experimental literature is available for relatively larger size droplets impacting and evaporating on hot surfaces (see, as an example, [1,2]). Evaporating (and moving) low temperature films have been widely analysed in icing problems [3,4] or shear and gravity driven water film motion [5], in presence of incoming water mass flow [4,5]. Less references can be found on the dynamics, condensation end evaporation of small scale dew droplets. A general review of the physical aspects of the dew formation is presented by Beysens [6], including a qualitative description of the droplet pattern evolution and coalescence processes during the growth of the dew layer. A theoretical analysis of the basic nucleation process, as well as experimental data extending to the frost nucleation, focused on the contact angle and supersaturation degree effects, has been given by Na and Webb [7]. The scattering of their experimental results reflects the high sensitivity of the phenomena on small perturbations. Numerical simulation of defogging phenomena in industrial application has been carried out in the automotive industry: however, the approach is significantly simplified, since droplet details are neglected [8] or taken into account in a simplified way [9], simply using a droplet radius rather then an average film height in the mass balance equations.

Here we present and validate a numerical procedure for the prediction of fogging-defogging processes. All the facets of the problem are handled via numerical analysis: air flow field, which define the convective heat and mass transfer from the misted glass to the environment, unsteady conduction within the solid glass, which has a major impact on the temperature rise speed, and water layer evolution. Although the simulation of the details of the water layer phenomena is extremely complex and sensitive to small perturbation (surface finiture, fouling, microscratching), some physical consideration will be used to derive a simplified but effective droplet evolution model.

2 Numerical procedure

In fig.1 we show a sketch of the physical problem for the windshield defogging simulation. We need a solution for the flow field inside the cabin, including the hot jets from the dashboard hot air outlets, in order to compute the inside heat and mass transfer coefficients. Then we have to define the proper mass and energy balances for the water layer, which should be properly modelled to include information from the actual droplet shape. A solution of the solid conduction problem is required to take into account thermal capacity and thermal resistence of the windshield glass, both in the normal and transverse directions. Finally, the evaluation of external side heat transfer coefficient will close the problem.

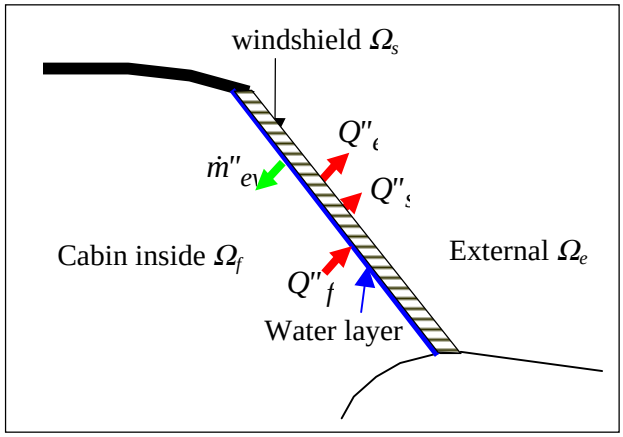

Fig.1 – Physical problem

The coupling between the different physical domains is obtained via an exchange of boundary conditions, allowing us to define the coupling as a purely interfacial algorithm, independent from the details of the solvers in the different domains. Thus, the described defogging procedure can be easily coupled with any commercial or proprietary computational code; here, CFX5.5 code was selected. Since the Poisson equation for the solution of the solid conduction problem is as a special case of the Navier-Stokes equations with zero velocities, the same flow code could be re-used to evaluate the solid temperature field [4]. However, in defogging applications the solid domain is typically limited to simple geometries like glass plates or windshields. Thus, a finite volume based code for structured meshes was used, taking advantage of its computational efficiency.

2.1 Conjugate heat transfer (CHT)

Flow solution is initiated with a guessed temperature distribution along the wall; the heat flux computed by the Navier-Stokes flow solver is then used as a boundary condition for the solid conduction problem, which then returns a new temperature profile on the wall. Neumann boundary condition are imposed on the solid and Dirichlet

ones on the fluid, on the basis of stability considerations [11]. The procedure for each time step can be summarized as follows:

1. fluid domain: solve Navier-Stokes and energy equations with Dirichlet b.c. at the interface Γ:

$$\begin{cases} f_f(T,v,p)=0 & on\ \Omega_f \\ T=T^k & on\ \Gamma \end{cases} \quad (1)$$

2. evaluate surface heat transfer on Γ
3. solid domain: solve the Poisson conduction equations with Neumann b.c. on Γ:

$$\begin{cases} f_s(T)=0 & on\ \Omega_s \\ \dfrac{\partial T}{\partial n}=-\dfrac{Q_s''}{k_s} & on\ \Gamma \end{cases} \quad (2)$$

4. evaluate surface temperature T_Γ on Γ
5. Fluid domain: update the Dirichlet b.c. on Γ
6. repeat until convergence of temperature.

The above mentioned procedure has proven successful for anti-icing and turbomachinery compressible flow applications [4,12,13] and for incompressible flow (decoupled thermal and flow field); strong coupling at each iteration implies that the number of time steps required for the CHT computation is of the same order as for a standalone computation. If an implicit algorithm is used for the fluid and conduction solvers, the lack of coupling linearization slightly reduces global convergence rate and stability, in comparison to the standalone computation. The use of Robin, rather than Neumann, conditions relaxes the problem:

$$\begin{cases} h=\dfrac{Q_s''}{T-T_0} & on\ \Gamma \\ f_s(T)=0 & on\ \Omega_s \\ \dfrac{\partial T}{\partial n}=-\dfrac{h(T-T_0)}{k_s} & on\ \Gamma \end{cases} \quad (3)$$

Furthermore, if temperature and velocity field are decoupled and the momentum equation time scale is much smaller than the energy equation one, as may happen for forced convection incompressible flow fogging problems, we can skip the flow computation step (1) using a distribution for heat transfer coefficient *h* from a single, off line, steady state flow field computation.

If temperature and velocities are coupled, as for natural convection, or if we follow a dynamic transient, full coupling is required.

2.2 Water layer mass and energy balance

Under fogging or defogging conditions evaporation or condensation of atmospheric humidity takes place on the solid surface. Thus, a transient balance of the water layer along the solid surface must be provided: the latent heat contribution will appear as an heat sink (evaporation) or source (condensation).

A very thin water layer, such as that on a fogged window, is composed by a collection of tiny droplets, rather than by a continuous film, and the surface tension at the droplets edge is strong enough to prevent shear or gravity driven flow along the surface. Thus, the mass balance includes only the evaporation or condensating mass flow, while no mass transfer occurs along the wall surface. Here, we adapted to these conditions a model originally developed for steady state icing and industrial problems [4,11].

The model is a 3D extension of the classical Messinger model. In our 3D Navier-Stokes context we take into account the film introducing a suitable heat sink at the interface between solid and flow domain. The film equation are solved on a 2D curvilinear mesh lying on the interface between the fluid and the solid, and each control volume on the interface is much larger than the droplet size. Neglecting the thermal and resistence capacity of the water layer, due to the small droplet size, the thermal balance of the interface control volume yields:

$$Q_s'' = Q_a'' \frac{A_{wet}}{A_t} + Q_a'' \frac{A_{dry}}{A_t} + \dot{m}_w'' \frac{A_{cap}}{A_t} \lambda(T_f) \quad (4)$$

where Q_s'' is the conduction heat flux per unit area from the solid, Q_a'' is the convective flux per unit area to the air, computed from the fluid solution, $\dot{m}_w''$ is the evaporating or condensating mass flow rate, λ is the evaporation latent heat, T_f the local interface temperature. Since the water layer is discontinuous, we must take into account different surfaces, as shown in fig.2: A_{wet} is the area of the droplet/solid interface, A_{dry} is the asrea of the dry portion of the solid surface, A_{cap} is the area of the droplet/fluid interface, here assumed as a spherical cap [1], A_t is the total area $A_t = A_{wet} + A_{dry}$. If H is the cell-averaged layer height, the mass balance yields:

$$\rho_w \frac{\partial H}{\partial t} = -\frac{A_{wet}}{A_t} \dot{m}_w'' \quad (5)$$

The maximum evaporation mass flow rate could be computed using either the proper transport equation or a heat and mass transfer analogy [14]:

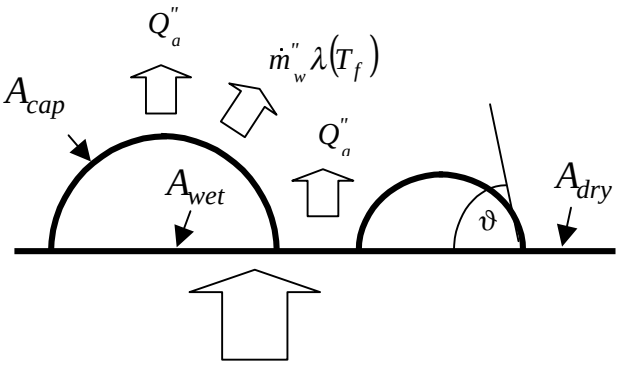

Fig. 2. Water layer: surfaces, contact angle ϑ, heat fluxes

$$\dot{m}''_w = \frac{h}{c_{p_{air}}}\left(\frac{Pr}{Sc}\right)^{\frac{2}{3}} \frac{M_{H_2O}}{M_{air}}\left(\frac{p_{s_f} - \phi_0\ p_{s_0}}{p_e - p_{s_f}}\right) \tag{6}$$

In eq.(6) the convective heat transfer coefficient h comes from the external flow solution and the last term involves the saturated steam pressure at film temperature p_{s_f}, and at freestream temperature p_{s_0}, the freestream pressure p_e and humidity ϕ_0. Saturation vapour pressure is given by:

$$p_s(T) = 2337 e^{\left[6789\left(\frac{1}{293.15} - \frac{1}{T}\right) - 5.03 ln\left(\frac{T}{293.15}\right)\right]} \tag{7}$$

The equation (6) is commonly accepted and holds true if the heat transfer scales with $Pr^{1/3}$, as often, although not always, happens [14]. In the present work we adopted the heat and mass transfer analogy. Eq. (4) provides the heat flux used as solid thermal boundary condition in the CHT procedure.

2.3 Droplet evolution

The geometry of the droplet has a fundamental impact on the misting process, since it defines the area ratios in Eq.(4). Assuming a spherical segment shape for the droplet, such geometry can be computed, for a given volume, from the contact angle between mist droplet and solid surface. However, the contact angle is not constant during the growing and evaporation process. If a cold surface, below dew point temperature, is exposed to a warm environment, nucleation of tiny condensing droplets occurs at the surface. The contact angle during this phase can be related to the advancing contact angle value, which is higher than the static and receding ones. When the droplets cover a significant part of the solid surface, coalescence between neighbouring ones will occur [6]. Since coalescence preserves volume, a release of free dry surface follows, allowing for new nucleation. This leads to self similarity in the droplet pattern [6], with a stabilization of the value of surface coverage similar to the one corresponding to close packing of small droplets. If the droplet or the substrate temperature rises above the dew point evaporation begins. Experimental evidences [2] show that during this phase the base area of the droplet is at first constant, and the contact angle decreases until the receding value is reached (see fig.2, t = 1,2,3,4). From this point on, the contact angle is preserved and the droplet volume reduction yields a wet area decrease (see fig.2, t = 5, 6).

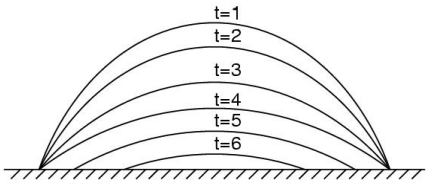

Fig. 3. Evaporation droplet shape evolution

In order to mimic these phenomena, during condensation we assume a contact angle equal to the advancing one, and compute a single representative base droplet diameter d corresponding to a closely packed distribution with an average cell-averaged height computed from eq.(5):

$$d = \frac{12\sqrt{3}(\sin\vartheta)^3 H}{\pi(1-\cos\vartheta)^2(2+\cos\vartheta)} \tag{8}$$

This diameter and the contact angle are used to evaluate the area ratios in eq.(4). During demist process we compute the droplet volume reduction from the height variation (eq.(5)) and obtain the new contact angle ϑ from the geometrical relationship

$$V = \frac{\pi}{3}\frac{(d/2)^3}{(\sin\vartheta)^3}(1-\cos\vartheta)^2(2+\cos\vartheta) \tag{9}$$

Actual ϑ will be the larger between the computed value and the assumed receding contact angle ϑ_r. If the computed value is lower then ϑ_r a new wet area A_{wet} will be computed from ϑ_r and droplet volume, yielding an increase in dry area.

3. Results and discussion

The simulation of the windshield defogging homologation tests of a FIAT Punto was chosen as an industrial test case. During the test the car is placed in a closed room at a constant temperature of -3°C. A steam generator introduces in the cabin a

steam mass flow rate of 350 g/h. Thus, the misting process occurs in a nearly still air environment.

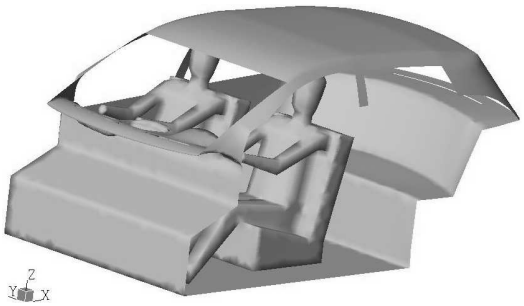

Fig.4 Physical domain

After five minutes the mass flow is reduced by 140 g/h and two passengers enter in the cabin. At this point, the engine and the defogging system are switched on. The defogging system blows hot air along the windshield, promoting the fogged layer evaporation. At fixed time interval the defogged region are recorded. Safety regulations impose that specified areas of the windshield are defogged within prescribed times.

The final defogging time is the result of the evolution of both a thermal and a dynamic transient. However, the time scale of the thermal problems are related to the thermal capacity of the windshield, of the air inside the cabin and the thermal inertia of the defogging system. Such time scale is of the order of the minutes. On the other hand, the dynamic time scale is related to the time required by the flow to run through the defogging system ducts and along the windshield. This is a much quicker process, with a time scale of a few seconds, and we should quickly achieve a steady state solution. Assuming uncompressible flow and neglecting buoyancy effects, the heat transfer coefficient should not depend on the temperature. Thus, we could consider a single steady state flow solution with arbitrary Dirichlet boundary condition along the glass, solving a transient problem only for the energy equation. Unfortunately, it is not possible to clearly define a reference temperature for the heat transfer coefficient: the inlet defogging air temperature is a good guess for the windshield area reached by the jet themselves, but the average cabin temperature drives the heat transfer in the regions far from the jets. Furthermore, the flow reaches a quasi-periodic regime, with unsteady large scale vortices growing in the rear part of the cabin (fig.5), rather than a steady condition. These oscillations have a relatively small effect on the flow structure near the windshield, but can affect the mixing of hot and cold air in the cabin and the average temperature.

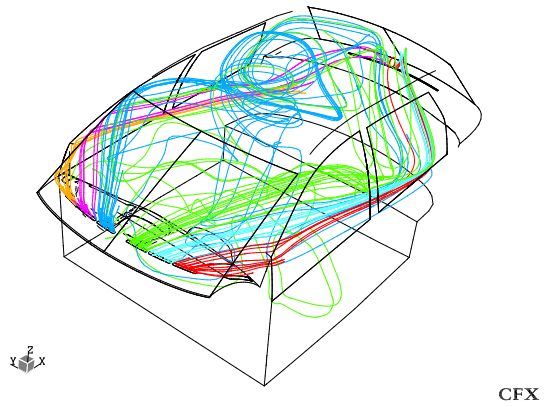

Figura 5. Cabin flowfield: streamlines

The unstructured mesh for the cabin (fig.6,7), refined near the windshield, has $7 \cdot 10^5$ cells. The use of the original CAD geometry ensured geometrical accuracy of the dashboard and of the ventilation system hot air outlets, while the rear of the cabin was simplified, thus sparing nodes and CPU time.

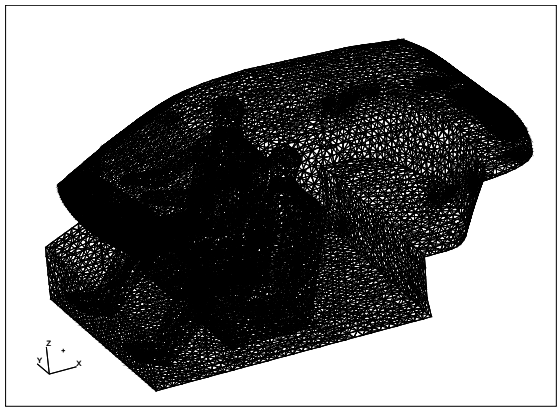

Fig. 6. Computational mesh

We simulated only the defogging process. The initial water layer thickness of *0.126mm* comes from literature suggestion, empirical correlations and water mass balance considerations. However, if required, the procedure can also compute the mist deposition process [15]. Even if the windshield is thin, with respect to the whole cabin, an accurate 3D solution of the conductive problem in the multilayer glass is essential. This is demonstrated in Fig.8, where we plot the temperature time history on the inner glass surface in a node close to the upper right windshield corner. Neglecting both the thermal resistance and capacity of the windshield glass we computed the case (a): the equilibrium temperature is reached in six minutes. In case (b) we took into account the glass thermal capacity, but we still neglected the transverse heat transfer through the glass, thus allowing a simple lumped parameters

modelling. Windshield warming process is slower, but still significantly shorter than the more accurate fully 3D prediction (line (c)).

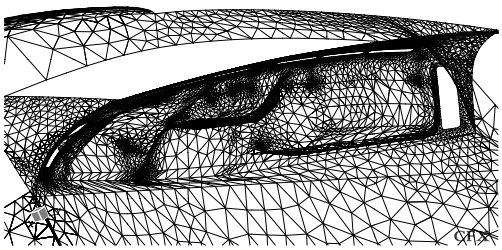

Fig. 7. Computational mesh: dashboard detail

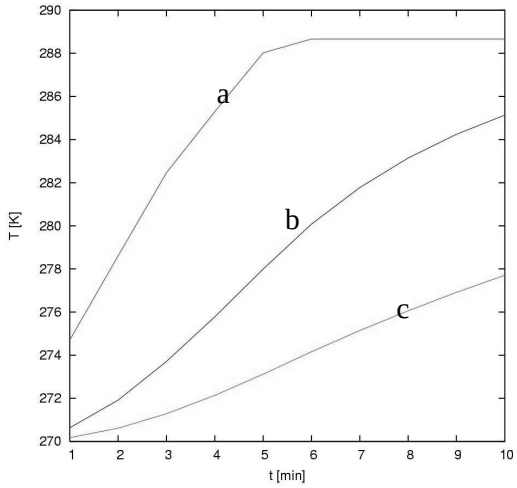

Fig. 8. Windshield temperature: (a) zero thermal capacity and thermal resistence; (b) no transverse conduction; (c) fully 3D glass temperature solution

Fig.9 compares the computed and experimental contour of the defogged area after two and four minutes from the defogging system start up, during a standard homologation test. The extension and position of the demisted area are satisfactorily predicted, while the actual shape of the clean area is a bit different. However, defogging phenomena are strongly influenced by a number of external factors (such as fouling). This yields significant uncertainity levels in the experimental data, as shown in [16]. It is worth notice that preliminary computations assuming a uniform film layer, rather than the discontinuous droplet layer, overestimated demisting time by 70%.

4. Conclusions

A numerical procedure for the prediction of transient defogging processes was described. The procedure computes the evolution of the water layer on an interface 2D grid, and the interaction with the flow solver is achieved through an exchange of boundary conditions.

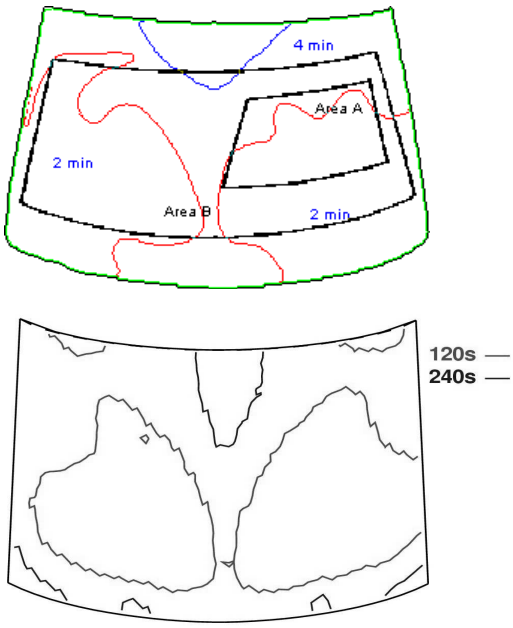

Fig. 9. Defogged surface: top, experimental data; bottom, computational results

Thus, a high level of flexibility is granted, both in the choice of the flow solver and in the degree of interaction between the solver and the water layer routines. In particular, one can perform an off line single computation of heat transfer coefficient if the thermal field is decoupled from the velocity ones. The phenomenological modelization of the mist droplet shape and evolution is able to mimic some of the effects of the contact angle on the demist speed, allowing the investigation of the effects of proper glass coatings. The procedure was validated through the simulation of an homologation defogging test for the automotive industry.

The flexibility of the computational approach suggest a wide range of future application, including optical and commercial refrigeration industry.

Nomenclature

A_{dry}	Dry solid area [m^2]
A_{wet} A_{cap}	Interface area, droplet/solid, droplet/air [m^2]
$c_{p_{air}}$	Air constant pressure specific heat [kJ/kgK]
d	Droplet base diameter [m]
h	Heat transfer coefficient [kW/m^2K]
H	Film call-averaged height [m]
k	Thermal conductivity [kW/mK]
m_w	Evaporating mass flow [kg/s]

M	Molecular weight [kg/kmol]
p	Static pressure [Pa]
Pr	Air Prandtl number
Q_s'' Q_a''	Conductive and convective heat flux [kW]
Sc	Air Schmidt number
t	Time [s]
T	Temperature [K]
ϑ	Contact angle
λ	Latent heat of evaporation [kJ/kg]
Ω_f, Ω_s	Fluid and solid domain
ρ,ρ_w	Solid density, water density [kg/m^3]
Γ	Solid - Fluid interface

References

[1] Chandra, S., di Marzo, M., Qiao, Y.M., Tartarini, P., Effect of liquid-solid Contact Angle on Droplet Evaporation, *Fire Safety Journal*, Vol. 27, pp 141-158, 1996.

[2] Crafton, E.F., Black, W.Z., Heat transfer and evaporation rates of small liquid droplets on heated horizontal surfaces, *Int. J. Heat and Mass Transfer*, Vol. 47, pp 1187-1200, 2004.

[3] Al-Khalil, K., Keith, T., De Witt, K., Modelling of Surface Water Behaviour on Ice Protected Aircraft Components, *Int. J. for Num. Meth. Heat and Fluid Flow*, Vol. 2, pp. 555-571, 1992

[4] Croce, G., Habashi, W.G., Thermal Analysis of Wing and Nacelle Anti-Icing Devices, *Computational Analysis of Convection Heat Transfer*, G. Comini and B. Sunden, Eds., WIT Press, Southampton, 2000

[5] Feddaoui, M., Mir A., Belahmidi E., Numerical simulation of mixed convection heat and mass transfer with liquid flm cooling along an insulated vertical channel, *Int. J. Heat and mass transfer*, Vol. 46, 2003

[6] Beysens, D., The formation of dew, *Atmospheric Research*, Vol.39, pp. 215-237, 1995

[7] Na, B., Webb, R.L., A fundamental understanding of factors affecting frost nucleation, *Int. J. Heat and Mass Transfer*, Vol.46, pp. 3797-3808, 2003

[8] Kitada M., Asano H., Kataoka T., Hirayama S., Numerical Analysis of Transient Defogging Pattern on Automobile, *SAE paper No. 2002-01-0223*, SAE World Congress and Ex., Detroit, 2002

[9] Hassan M.B., Petitjean C., Deffieux J.C., Gilotte P., Windshield Deffoging Simulation with Comparison to Test Data, *SAE paper No. 1999-01-1202*, SAE International Congress and Ex., Detroit, 1999

[10] Giles, M.B., Stability in Analysis of Numerical Interface Conditions in Fluid-Structure Thermal Analysis, *Int. J. for Num. Meth. in Fluids*, vol. 25, pp. 421-436, 1997

[11] Croce, G., Beaugendre, H., Habashi, W.G., 2002, Numerical simulation of heat transfer in mist flows, *Num.l Heat Transfer*, Vol. 42, pp. 139-152

[12] Croce, G. A Conjugate Heat Transfer Procedure for Gas Turbine Blades, in Heat Transfer in Gas Turbine Systems, *Annals of N.Y. Academy of Sciences*, vol. 934, pp 273-280, 2001.

[13] Chen, Y., Fiebig, M., and Mitra, N.K., "Conjugate Heat Transfer of a Finned Oval Tube. Part A: Flow Patterns", *Num. Heat Transfer*, Part A, vol. 33 n.4, pp. 371-385, 1998.

[14] G. Comini, G. Croce, "Convective heat and mass transfer in tube-fin exchangers under dehumidifying conditions", *Num. Heat Transfer, Part A*, Vol. 40, pp. 579-599, 2001

[15] G. Croce, P. D'Agaro, F. Della Mora, "Numerical simulation of glass fogging and defogging", CHT04, Int. Symp. On Advances Comp. Heat Transfer, Norway 2004

[16] Margrain T.H., Owen C., The misting characterstics of spectacle lens, *Ophthal. Physiol. Opt.* Vol.16 No.2, pp.108-114, 1996